



## The usefulness of short-term high-fat/high salt diet as a model of metabolic syndrome in mice



Leônidas Graças Mendes-Junior<sup>a,1</sup>, Leandro Ceotto Freitas-Lima<sup>b,1</sup>, Janaína Ribeiro Oliveira<sup>b</sup>, Marcos B. Melo<sup>e</sup>, Jonh David Feltenberger<sup>d</sup>, Igor Viana Brandi<sup>b</sup>, Bruna Mara Aparecida Carvalho<sup>b</sup>, André Luiz Sena Guimarães<sup>c</sup>, Alfredo Maurício Batista De Paula<sup>c</sup>, Carlos Eduardo Mendes D'Angelis<sup>c</sup>, Maria José Campagnole-Santos<sup>e</sup>, Robson Augusto Souza Santos<sup>e</sup>, Valdir Andrade Braga<sup>a</sup>, Sérgio Henrique Sousa Santos<sup>b,c,\*</sup>

<sup>a</sup> Department of Biotechnology, Biotechnology Center, Federal University of Paraíba, João Pessoa, PB, Brazil

<sup>b</sup> Institute of Agricultural Sciences, Food Engineering College, Universidade Federal de Minas Gerais (UFMG), Montes Claros, Minas Gerais, Brazil

<sup>c</sup> Lab. Health Science, PPGCS, Universidade Estadual de Montes Claros (Unimontes), Minas Gerais, Brazil

<sup>d</sup> Medical School, Touro University, Las Vegas, USA

<sup>e</sup> Physiology Department, Universidade Federal de Minas Gerais (UFMG), Belo Horizonte, Minas Gerais, Brazil.

### ARTICLE INFO

#### Keywords:

Metabolic syndrome  
Animal model  
Mice  
Obesity  
Heart

### ABSTRACT

Diabetic cardiomyopathy (DC) describes diabetes-associated changes in the structure and function of myocardium that are not directly linked to other factors such as hypertension. Currently there are some models of DC; however, they take a large time period to mimic key features. In the present study, we investigated the effects of a short-term high-fat/high salt diet (HFHS) treatment on myocardial function and structure, and vascular reactivity in C57BL/6 male mice. After 14 weeks HFHS induced hypertension (MAP =  $144.95 \pm 16.13$  vs  $92.90 \pm 18.95$  mm Hg), low glucose tolerance (AUC =  $1049.01 \pm 74.79$  vs  $710.50 \pm 52.57$  a.u.), decreased insulin sensitivity (AUC =  $429.83 \pm 35.22$  vs  $313.67 \pm 19.55$  a.u.) and increased adiposity (epididymal fat weight  $0.96 \pm 0.10$  vs  $0.59 \pm 0.06$  OW/BW  $\times 10^2$ ), aspects present in metabolic syndrome. Cardiac evaluation showed diastolic dysfunction (E/A ratio =  $1.20$  vs  $1.90$  u.a.) and cardiomyocyte hypertrophy (cardiomyocyte area =  $502.82 \pm 31.46$  vs  $385.58 \pm 22.11$   $\mu\text{m}^2$ ). Lastly, vascular reactivity was impaired with higher contractile response ( $136.10 \pm 3.49$  vs  $120.37 \pm 5.43\%$ ) and lower response to endothelium-dependent vasorelaxation ( $74.01 \pm 4.35$  vs  $104.84 \pm 3.57\%$ ). In addition, the diet was able to induce an inward coronary remodeling (vascular total area: SCNS  $6185 \pm 800.6$  vs HFHS  $4085 \pm 213.7$   $\mu\text{m}^2$ ). Therefore, we conclude that HFHS short-term treatment was able to induce metabolic syndrome-like state, cardiomyopathy and vascular injury working as an important tool to study cardiometabolic diseases.

### 1. Introduction

Diabetes mellitus (DM) reduces life expectancy as a major cause of complications such as renal failure, ischemia and myocardial infarction [1]. Some important studies reveal that vascular complications of DM are associated with multiple risk factors, such as obesity, hyperlipidemia, hyperglycemia and hypertension, parameters found in the metabolic syndrome [1–3].

Diabetic cardiomyopathy (DCM) is recognized by impaired

myocardial relaxation, left ventricular stiffening, progressive development of interstitial fibrosis and cardiomyocyte hypertrophy. Although diabetes experimental animal models are extensively used in the literature and diabetic cardiomyopathy is known as a progressive disease that begins early in the diabetes onset, the natural history and progression of DCM has never been directly studied [4].

It has been showed in a few studies that a diet rich in macronutrients such as lipids and carbohydrates contribute to cardiometabolic alterations, via increased adiposity, cholesterol and glycemic

\* Corresponding author at: Institute of Agricultural Sciences, Food Engineering College, Universidade Federal de Minas Gerais (UFMG), Avenida Universitária, 1.000 – Universitário, 39, 404-547 Montes Claros, MG, Brazil.

E-mail address: [sergiosousas@hotmail.com](mailto:sergiosousas@hotmail.com) (S.H.S. Santos).

<sup>1</sup> Equally contributed to this study.

<https://doi.org/10.1016/j.lfs.2018.08.034>

Received 20 June 2018; Received in revised form 10 August 2018; Accepted 12 August 2018

Available online 14 August 2018

0024-3205/ © 2018 Elsevier Inc. All rights reserved.

levels [5]. However, these diets do not induce representative alterations of cardiovascular dysfunctions as verified in cardiomyopathy [6]. Yu and cols [7], tested different diets with high-salt content and observed dysfunctions in the ventricular dynamics, hindering blood ejection force, which is common in cardiomyopathy [8]. However, the long-term treatment required in the presented models, which varies from 20 to 30 weeks, represents an important limitation.

In this perspective, we aimed to evaluate the cardiovascular damage of a high-fat/high-salt diet as well as the metabolic profile in mice.

## 2. Methods

### 2.1. Animals and protocols

Twenty male C57BL/6 mice (four-week-old) from the Federal University of the Minas Gerais (Belo Horizonte, Minas Gerais, Brazil) were kept under standard conditions (12 h light/dark cycles,  $21 \pm 2^\circ\text{C}$ ) and with free access to chow and water. All procedures complied with both the standards stated in the Guide for the National Institutes of Health guide for the care and use of Laboratory animals (NIH Publications No. 8023, revised 1978) and the Care and Use of Laboratory animals (Institute of Laboratory Animal Resources, National Academy of Sciences, Bethesda, Md, 1996) and were conducted under conditions approved by the local animal ethics committee, CETEA/UFMG.

Mice were randomly divided into two groups: standard chow/normal salt diet (NCNS), composed of 66.0% carbohydrate, 23.0% protein, 11.0% fat and 0.2% NaCl, presenting a total of 9.13 kJ/g (Labina-Purina®, Brazil). High-fat chow/high-salt diet (HFHS) was composed of 26.0% carbohydrate, 14.0% protein, 60.0% fat (50% from lard and 10% from soybean oil) and 7.25% NaCl, presenting a total of 23.38 kJ/g. Both groups were fed respective experimental diets for 14 weeks.

### 2.2. Measurements of body weight, food intake and tissue collection

We measured body weight (BW) and food intake once and twice, respectively, each week during the treatment. After 14 weeks of treatment mice were killed by decapitation and samples of heart; epididymal, retroperitoneal and mesenteric white adipose tissue were collected and weighed to determine the organ weight (OW). Data was expressed as  $\text{OW}/\text{BW} \times 10^2$ .

### 2.3. Glucose tolerance and insulin sensitivity tests

The intraperitoneal glucose tolerance tests (IPGTT) and intraperitoneal insulin tolerance test (IPITT) were performed in all animals of each group as described previously [37]. Briefly, D-glucose (2 mg/g body weight, ip) was injected into overnight fasted mice. Glucose levels from tail blood samples were monitored at 0, 15, 30, 60, and 90 min after injection using an Accu-Check glucometer (Roche-Diagnostics®, Indianapolis, USA). Insulin sensitivity test was performed on overnight-fed mice, after intraperitoneal injection of insulin (0.75 units/kg body weight; Sigma–Aldrich®, St. Louis, USA). Tail blood samples were taken at times 0, 30, 60, 90 and 120 min after injection for measurement of blood glucose levels. Both tests were performed in the last week of treatment.

### 2.4. Blood pressure measurements

Arterial blood pressure was measured in conscious mice at week 13 using a computerized and non-invasive tail-cuff system (CODATM system, Kent Scientific) following the original protocol described by Daugherty [38]. In order to habituate the animals to the device and reduce variations in response to stress, arterial blood pressure measurements were carried out daily for one week just prior to the

experiment. The first five cycles were discarded and the average of the 15 subsequent arterial blood pressure measurement cycles was used. We performed arterial blood pressure measurements between 2:00–5:00 pm [38].

### 2.5. Isometric tension measurement

We obtained rings ( $\approx 2$  mm) from the descending thoracic aorta, free of adipose and connective tissue from mice immediately after sacrifice. We placed these rings in Krebs-Henseleit solution with the following composition (mM/L): NaCl 110.8, KCl 5.9,  $\text{NaHCO}_3$  25.0,  $\text{MgSO}_4$  1.07,  $\text{CaCl}_2$  2.49,  $\text{NaH}_2\text{PO}_4$  2.33, and glucose 11.51, at  $37^\circ\text{C}$ , pH of 7.4, under a tension of 0.5 g, for 1 h for equilibration. The presence of a functional endothelium was assessed by the ability of acetylcholine (ACh) ( $10^{-5}$  M; Sigma-Aldrich®) to induce  $> 70\%$  relaxation of vessels precontracted with phenylephrine (Phe) ( $10^{-5}$  M; Sigma-Aldrich®). In all experiments, the aortic rings were exposed twice to depolarizing Krebs-Henseleit solution ( $\text{K}^+$  60 mM). After washout, the contractile responses to Phe or relaxation responses to ACh and sodium nitroprusside (SNP) were recorded. A concentration-response curve to Phe was recorded as percentage of the maximum contraction obtained following tissue stimulation with high  $\text{K}^+$  using half-log concentration increments ( $10^{-9}$ – $10^{-5}$  M). Increasing concentrations of ACh ( $10^{-10}$ – $10^{-5}$  M) or SNP ( $10^{-11}$ – $10^{-6}$  M) were administered at half-log increments to evaluate endothelium dependent and independent vasorelaxation, respectively. A selective cyclo-oxygenase inhibitor, indomethacin ( $10^{-6}$  M), was added to the Krebs' solution 30 min before the construction of a concentration–response curve. The drug-induced responses were measured using the MacLab Chart v 7.2.1 program (AD Instruments, Australia).

### 2.6. Echocardiographic analysis

Transthoracic echocardiographic examination was performed in mice using a high-frequency, high-resolution echocardiographic system consisting of a VEVO 2100 ultrasound machine equipped with a 30–40 MHz bifrequencial transducer (Visual Sonics, Toronto, Canada). Anesthesia was induced in mice with 5% isoflurane and maintained via a nose cone with 1.25% isoflurane. The anterior chest was shaved and the mice were placed in supine position on an imaging stage equipped with built-in electrocardiographic electrodes for continuous heart rate monitoring and a heater to maintain body temperature at  $37^\circ\text{C}$ . High-resolution images were obtained in the right and left parasternal long and short axes and apical orientations. Standard B-mode images of the heart and pulsed Doppler images of the mitral and tricuspid inflow were acquired. Left ventricular dimensions and wall thickness were measured at the level of the papillary muscles in left and right parasternal short axis during the end systole and end diastole. Left ventricular ejection fraction, fractional shortening, and mass were measured. All the measurements and calculations were done in accordance with the American Society of Echocardiography. The following M-mode measurements were performed: ventricular internal dimensions at diastole (LVIDD), left ventricular internal dimensions at systole (LVIDS), left ventricular posterior wall dimensions at diastole (LVPWD), left ventricular posterior wall dimensions at systole (LVPWS), interventricular septal dimensions at diastole (IVSDD) and interventricular septal dimensions at systole (IVSDS). Based on these parameters the diastolic left ventricular volumes (EDLVV), systolic left ventricular volumes (ESLVV), fractional shortening (FS), left ventricular ejection fraction (EF), stroke volume (SV), and cardiac output (CO) were calculated. Also, the radial strain from the bidimensional long axis view of the left ventricle was performed using the Vevostain software. The following parameters were evaluated: velocity, displacement, strain, and strain rate the E/A ratio was derived using the pulse wave Doppler recording of mitral valve leaflet tips provides mitral inflow velocity patterns from which early diastolic velocity (E), late diastolic velocity with diastolic

contraction (A).

## 2.7. Histological analysis of cardiac hypertrophy

Hearts were collected, fixed in 4% (v/v) paraformaldehyde (PBS-buffered), dehydrated, and embedded in paraffin. Heart sections (5  $\mu$ m in thickness) were stained with hematoxylin and eosin (H&E). Images of the heart (n = 4/5 per group) were captured using a 40 $\times$  objective with a colour video camera (VKC150, Hitachi, Tokyo, Japan) connected to a microscope (Olympus AX70, Olympus, Center Valley, PA, USA) and analysed using an Image ProPlus 7.0. Cell area was quantified in at least 40 myocytes in five visual fields.

## 2.8. Statistical analysis

Analyses were performed using the GraphPad Prism 5.0 software. Results are presented as the mean  $\pm$  SEM. Comparisons between two groups were carried out using Student *t*-test. Two-way ANOVA was used for graph lines to verify the interaction between the independent variables time and strain and was followed by Bonferroni post-test and *p* values < 0.05 were considered significant.

## 3. Results

### 3.1. Body composition and food intake

The animals of both groups started with similar body weight (SCNS = 10.20  $\pm$  1.75 vs HFHS = 10.40  $\pm$  1.64 g). The high-fat diet intake did not induce larger body mass gains (18.30  $\pm$  0.51 g) compared to standard chow body mass gains (18.40  $\pm$  0.50 g, Fig. 1A). Similarly, final body weight was also similar (SCNS = 28.60  $\pm$  1.77 vs HFHS = 28.70  $\pm$  1.94 g). On the other hand, animals of different groups showed different feeding behavior; Animals from HFHS group presented lower food intake (0.55  $\pm$  0.03 vs 0.92  $\pm$  0.07 g/day/mice, *p* < 0.05, Fig. 1B) and a higher energy intake (13.00  $\pm$  0.72 kJ/day/mice, *p* < 0.05, Fig. 1C) compared to SCNS group, respectively.

Additionally, the adipose tissue analysis revealed a higher epididymal adipose tissue weight (Fig. 1D) in HFHS group (0.96  $\pm$  0.10 OW/BW  $\times$  10<sup>2</sup>) than SCNS group (0.59  $\pm$  0.06 OW/BW  $\times$  10<sup>2</sup>, *p* < 0.05), the other areas remained unchanged, as well as other organs examined (data not shown).

### 3.2. Glucose tolerance and insulin sensitivity tests

The HFHS group presented a low glucose tolerance profile (Fig. 2A); 15, 30, and 60 min after D-glucose injection the blood glucose was higher (333.50  $\pm$  24.62; 352.17  $\pm$  36.53 and 242.17  $\pm$  14.17 mg/dL, respectively) than SCNS group (227.00  $\pm$  23.27; 206.43  $\pm$  19.89 and 156.14  $\pm$  8.27 mg/dL, respectively), resulting in an increased AUC (1049.01  $\pm$  74.79 vs 710.50  $\pm$  52.57 a.u., Fig. 2B). Moreover, decreased insulin sensitivity was observed in HFHS mice compared with the standard chow group (Fig. 2C), the curve shows higher glucose

values in the last three times (102.83  $\pm$  9.55; 110.50  $\pm$  9.31 and 126.50  $\pm$  6.78 mg/dL, respectively) than the SCNS group (58.67  $\pm$  3.53; 67.33  $\pm$  9.27 and 74.16  $\pm$  9.17 mg/dL, respectively) as well as a higher AUC (429.83  $\pm$  35.22 vs 313.67  $\pm$  19.55 a.u.) as shown in Fig. 2D.

### 3.3. Blood pressure

After 14 weeks of diet treatment the animals of HFHS group had a high systolic (176.00  $\pm$  18.91 mm Hg) and diastolic (128.57  $\pm$  16.95 mm Hg) blood pressure and consequently a high mean blood pressure (144.95  $\pm$  16.13 mm Hg) than the SCNS group (119.13  $\pm$  17.50; 79.95  $\pm$  18.71; 92.90  $\pm$  18.95 mm Hg, respectively, *p* < 0.05, Fig. 3).

### 3.4. Cardiac analysis

The echocardiographic examination showed an alteration on E/A ratio (Fig. 4A); while the SCNS group presented 1.90  $\pm$  0.19 and HFHS group ratio was 1.20  $\pm$  0.11, a significant decrease (*p* < 0.05). Despite the decrease in cardiac output (Fig. 4B) of HFHS group the change was not significant compared to SCNS group. Similar results were found in the analysis of left ventricle end-diastolic and end-systolic diameter (Fig. 4C and D). The analysis of left ventricular end-diastolic and end-systolic posterior wall dimension showed an increase in both (Fig. 4E and F), but only in end-systole was the HFHS significantly different from the SCNS group (1.20  $\pm$  0.06 vs 1.05  $\pm$  0.022 mm, respectively, *p* < 0.05). Left ventricular end-diastolic and end-systolic volumes are also not changed by HFHS feed (Figs. 4G and H, 5).

Histological findings suggest abnormalities in the heart. Cardiomyocytes area of left ventricular tissue in HFHS group (502.82  $\pm$  31.46  $\mu$ m<sup>2</sup>) was substantially greater when compared to the SCNS group (385.58  $\pm$  22.11  $\mu$ m<sup>2</sup>, *p* < 0.05, Fig. 6B). Additionally, in HFHS mice, the left ventricular internal diameter was increasing, however not different to control group; similarly, the left ventricle wall was similar for both groups (Fig. 6C and D). It is important to note an excessive presence enlarged nuclei, as occur in cardiac hypertrophy (Fig. 6A).

### 3.5. Vascular reactivity

The vascular response assessed in rings with functional endothelium using Phe (10<sup>-9</sup>–10<sup>-5</sup> M) are illustrated in Fig. 7A. In the HFHS group the maximum effect of Phe was increased compared to SCNS group (136.10  $\pm$  3.49 vs 120.37  $\pm$  5.43%, respectively, *p* < 0.05) as well as the potency indicated by pD<sub>2</sub> (6.85  $\pm$  0.03 vs 6.49  $\pm$  0.04 respectively, *p* < 0.05). Furthermore, HFHS group showed a decrease in relaxation induced by Ach (Fig. 7B), as shown by the lower value of E<sub>max</sub> = 74.01  $\pm$  4.35% and pD<sub>2</sub> = 7.09  $\pm$  0.08 when compared to SCNS (E<sub>max</sub> = 104.84  $\pm$  3.57% pD<sub>2</sub> = 7.36  $\pm$  0.04). The concentration-response curve to SNP was similar to in both groups (data not shown).

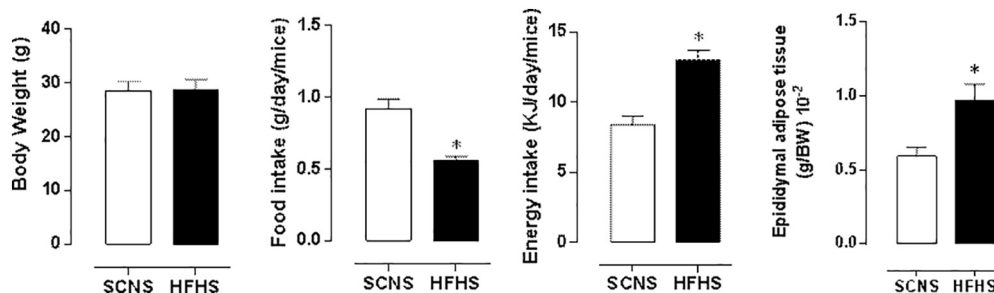


Fig. 1. Body profile. Data are shown as means  $\pm$  SEM. \**p* < 0.05 when compared to SCNS. SCNS: standard chow/normal salt diet (n = 6). HFHS: Short-term high-fat/high salt diet (n = 7).

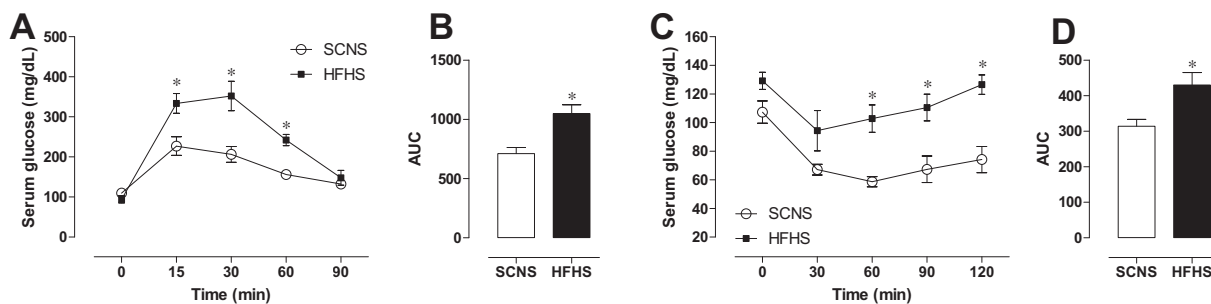


Fig. 2. (A) Glucose tolerance test and (B) insulin sensitivity test. Data are presented as means ± SEM. \**p* < 0.05 when compared to SCNS. SCNS: standard chow/normal salt diet (n = 6). HFHS: short-term high-fat/high salt diet (n = 7).

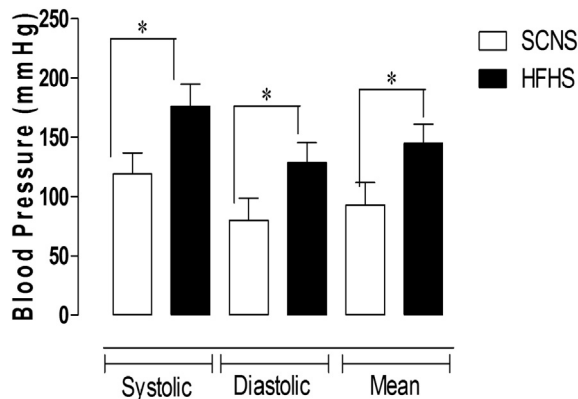


Fig. 3. Blood pressure compared at the end of treatment. Data are presented as means ± SEM. \**p* < 0.05 when compared to SCNS. SCNS: standard chow/normal salt diet (n = 6). HFHS: short-term high-fat/high salt diet (n = 7).

#### 4. Discussion

The main findings of the present study reported that a short high-fat/high-salt chow treatment was able to induce a characteristic profile of metabolic syndrome, including hypertension, low glucose tolerance, decreased insulin sensitivity and increased adiposity. Indeed, the cardiovascular functional analyses revealed a decreased E/A ratio and damage to vascular reactivity.

The main findings of the present study exemplify the progression of the diabetic cardiomyopathy disease alterations. These findings might be justified by the high-fat diet effects, which induces body weight gain and consequently increased adiposity. An increased body fat mass promotes the exacerbated secretion of adipokines that are correlated with insulin resistance, glucose tolerance as well as the specific tissue alterations found in metabolic syndrome [9]. Cardiac muscle alterations may also be observed, thus explaining the increasing number of cardiomyopathies [10].

In this context, the use of experimental models are needed for the treatments comprehension and propositions. There is a variety of

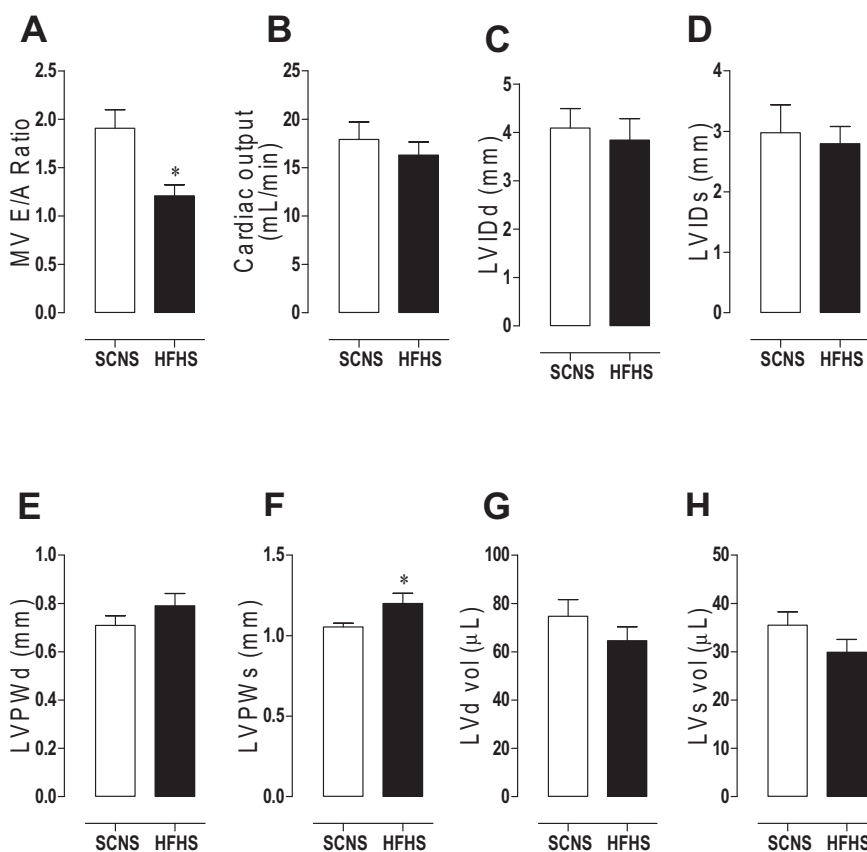
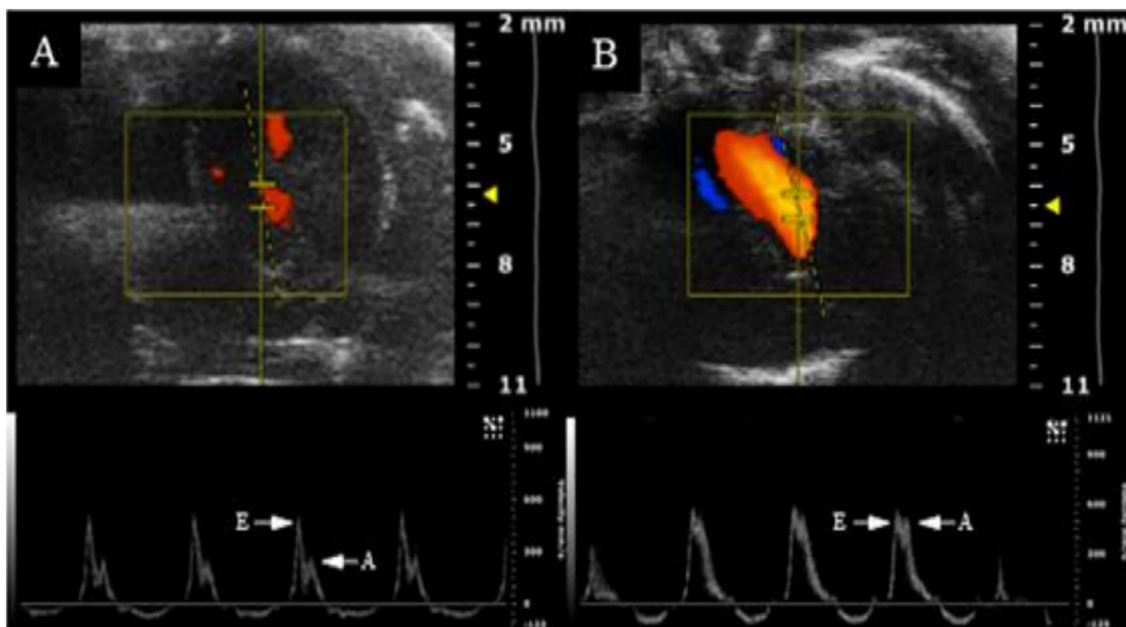


Fig. 4. Echocardiographic analysis in SCNS and HFHS groups. (A) Evaluation of mitral valve function, early (E) wave/atrial (A) wave ratio. (B) Cardiac output. (C) Left ventricle end-diastolic diameter. (D) Left ventricle end-systolic diameter. (E) Left ventricle posterior wall end-diastole diameter. (F) Left ventricle posterior wall end-systole diameter. (G) Left ventricle end-diastole volume. (H) Left ventricle end-diastole volume. Data are presented as means ± SEM. \**p* < 0.05 when compared to SCNS. SCNS: standard chow/normal salt diet (n = 6). HFHS: short-term high-fat/high salt diet (n = 7).



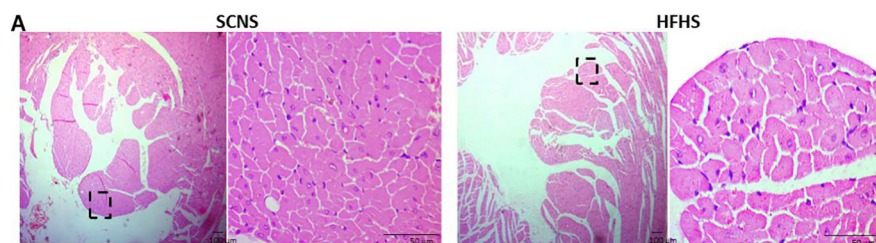


**Fig. 5.** Representative transmitral pulsed-wave Doppler of a (A) SCNS animal, showing a normal early (E) and late (A) mitral valve inflow waves and a (B) HFHS animal with an abnormal early (E) and late (A) mitral valve inflow waves. SCNS: standard chow/normal salt diet (n = 6). HFHS: short-term high-fat/high salt diet (n = 7).

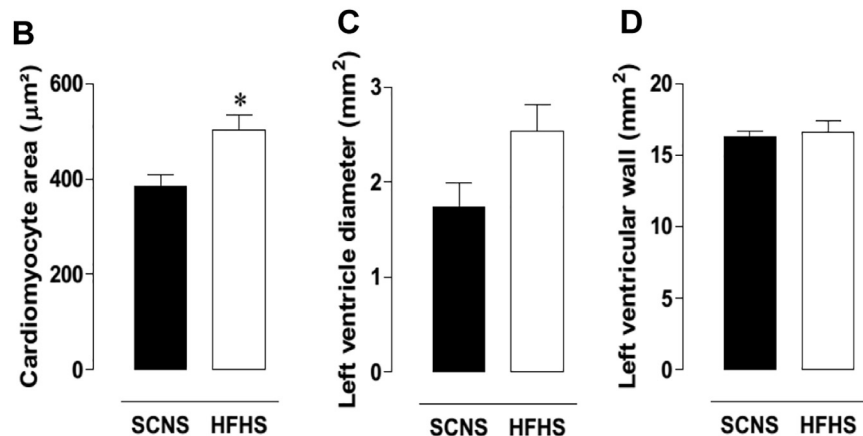
animals with genetic-specific (Knockouts) or high-fat and high-carbohydrate diets-induced alterations. However, these models have limitations, such as the specificity of alterations found in genetically modified experimental animals and the high-macronutrients content in diet-induced models, besides the fact that several models do not induce a satisfied number of dysfunctions, such as cardiovascular [11]. On the other hand, high-salt diets lead to cardiac hypertrophy elevated systolic blood pressure and cardiac dysfunction; furthermore, they induce arterial wall thickening, collagen and fibronectin deposition, as well as

the hypertrophy of vascular smooth muscle cells (VSMC). All these changes affect arterial structure and function by altering the characteristics of VSMC and endothelial cells [12,13]. However, the induction time is very long, varying from 20 to 30 weeks, in addition to the very high-NaCl levels observed [5,6]. In the present study the characterization of the high-fat and salt model evidenced alterations in the biophysical, glycemic cardiac and endothelial profiles after 14 days of treatment with a high-fat diet enriched with 7.25% of salt.

Nevertheless, we observed small increase in the deposition of



**Fig. 6.** Histological analysis of cardiac morphology. (A) Top panel microphotographs are typical cross-sections of heart of SCNS and HFHS mice (B) cardiomyocyte area from SCNS and HFHS group. (C) and (D) Left ventricle (lumen) diameter and wall thickness, respectively. Data are presented as means ± SEM. \**p* < 0.05 when compared to SCNS. SCNS: standard chow/normal salt diet (n = 6). HFHS: short-term high-fat/high salt diet (n = 7).



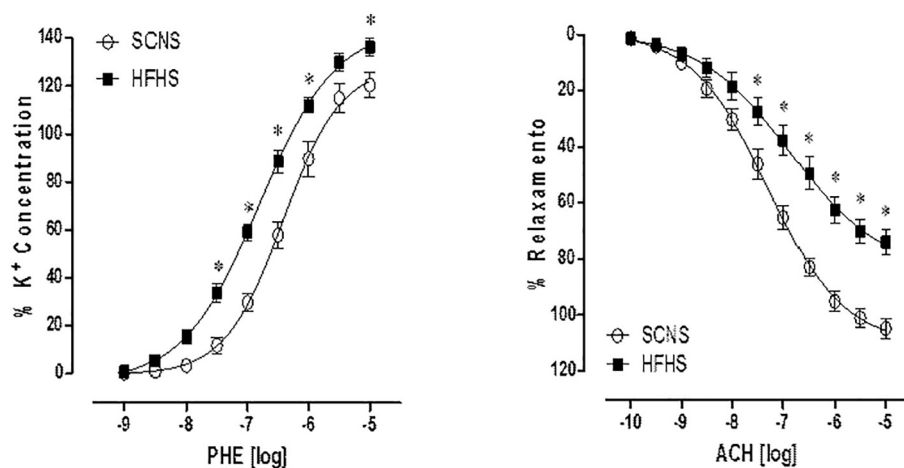


Fig. 7. Evaluation of vascular reactivity in aorta artery rings. (A) Concentration–response curve to Phe and (B) concentration–response curve for Ach in rings with functional endothelium. Data are presented as means  $\pm$  SEM. \* $p < 0.05$  when compared to SCNS. SCNS: standard chow/normal salt diet ( $n = 6$ ). HFHS: Short-term high-fat/high salt diet ( $n = 7$ ).

visceral fat in animals treated with high-fat/salt diet. Considering that the HFHS diets has a significantly higher energy value than the SCNS diet, the consumption of the saturated fat diet was slightly lower, although not enough to compensate, resulting in higher energy consumption in the HFHS group. Hypertension is another key feature in metabolic syndrome and the role of insulin in regulating blood pressure has been demonstrated. Initially, insulin resistance was directly correlated with the severity of hypertension [14]. Furthermore, insulin resistance can lead to the development of hypertension by impairing vasodilation induced by nitric oxide [15]. In addition, insulin also increases the activity of the sympathetic nervous system [16]. Lastly, fatty acids themselves can mediate relative vasoconstriction [17]. Clearly, there is sufficient evidence that metabolic changes are linked to hypertension; however, few studies have focused on hypertension as the possible cause for these metabolism alterations. Moreover, hypertension models have shown drawbacks, high-fat diets, for example, have variable effects on C57BL/6J mice and can neither induce alterations on blood pressure nor induce slight increases (10–15 mm Hg) [18].

Both high-fat diets and diets rich in salt induce cardiac morpho-functional modifications [19]. Myocardial metabolic remodeling plays a key role in cardiac diseases, as do ventricular hypertrophy and diabetic cardiomyopathy. Despite its complexity, few studies have tried to unravel the mechanism by which diabetes affects the morphology and structure of the heart. Some reports link type 2 diabetes to a disproportionate increase in left ventricular wall mass [20,21]. A few studies have also investigated the Epicardial Adipose Tissue (EPA) in experimental animal models, although scarce in the literature. The EPA influence on cardiovascular dysfunction has been pointed in the literature [22,23]. We believe that this tissue may possibly have influence on diabetic cardiomyopathy, although more specific studies should be performed to clarify this relationship.

Regarding salt diets, some studies show cardiomyocyte hypertrophy and interstitial fibrosis occurring independently of the effect on arterial blood pressure, and possibly due to cardiac Renin-Angiotensin System activation [24]. Several studies have pointed out the evidence of left ventricular remodeling and hypertrophy in diabetes mellitus, irrespective of the coexistence of concomitant risk factors. Besides, the former has been described as an early sign of this diabetic diastolic dysfunction heart muscle disease preceding the systolic damage [25].

Echocardiography is well known as a noninvasive and inexpensive tool to evaluate changes in heart structure/function that are echogenic. Using the mitral valve blood inflow, it is possible to measure the diastolic function in the heart through a pulsed-wave Doppler, also known as transmitral Doppler. Transmitral Doppler generates several indices for the analysis of diastolic function, using blood flow characteristics of high frequency and low amplitude [26]. Among all variables derived

from transmitral Doppler, we highlight the early ventricular filling wave (E-wave) and late ventricular filling wave (A-wave), reported as the E/A ratio. In addition to this parameter, the isovolumic relaxation time, E-wave peak velocity, E-wave deceleration time and A-wave duration can also be extracted [27]. The results obtained from the HFHS diet showed a considerable decrease in the E/A ratio, which results from an early decrease and late increase in diastolic flow, a characteristic of diastolic dysfunction and an early manifestation of diabetes mellitus in the myocardium [26].

In type 2 diabetes models, diabetic cardiomyopathy is characterized by early impairments in diastolic dysfunction, but it is also accompanied by structural abnormalities such as cardiomyocyte hypertrophy, myocardial fibrosis, and increased cardiomyocyte apoptosis [28]. Our results also match previous findings; the HFHS diet induces an increase in the cardiomyocyte area, but no changes in other parameters [29]. In addition, Candemir et al. found in their work that negative remodeling was more prevalent in diabetic patients and Delbin and Trask, found in their study that models of diabetes and metabolic syndrome that coronary arteries showed inward hypertrophic remodeling [30,31]. However, we consider diet combination to contribute to the deleterious effects found on the heart. Thus, the all of the cardiac analyses indicate that treatment with the HFHS diet, even for a short period (14 weeks) was able to induce major findings of diabetic cardiomyopathy, such as diastolic dysfunction and cardiomyocyte hypertrophy.

High-fat diet models as well as obesity have been implicated in the increase of endothelial vasoconstrictors and growth factors ET-1, prostanoid endothelium-derived vasoconstriction factor/thromboxane A<sub>2</sub>/prostaglandin H<sub>2</sub> (EDCF), angiotensin II (Ang II) and superoxide anion, which lead to endothelial dysfunction, oxidant stress, and stroke in multiple experimental models and in human populations. It has also been demonstrated that endothelial dysfunction contributes to the development of hypertension in high-fat diet models [32].

High-salt diet is known to induce and maintain hypertension in animal models of hypertension and in humans, on which the main contributor to its genesis is the endothelial dysfunction, in particular the altered vascular reactivity due to impairment in NO production. Also, an increased superoxide production occurs in vasculature, resulting in increased oxidative stress and reduced NO bioavailability [33].

In fact, the results of this study support the evidence that diets containing high levels of NaCl induce sustained increases in blood pressure. Furthermore, Phe induced contraction of rings of the HFHS group, in a more intense way and with maximum effect compared with the SCNS group. Vascular remodeling has been reported as a potential cause of increase of vascular reactivity to  $\alpha$ 1-adrenergic receptor agonists, involving a decrease of endothelium-derived relaxing factor NO as well as overexpression of proteins and receptors on the vascular smooth

muscle related to contraction [34,35]. At the same time, HFHS diet treatment leads to a reduction in relaxation induced by Ach, a muscarinic agonist receptor. These receptors are present in the vascular endothelium and their activation culminates in the release of NO. Thus, the reduction in the maximum effect and potency of ACH observed in this work means an impairment of NO bioavailability.

The main findings reported in the present study might contribute to the understating of cardiomyopathy-associated factors evolution, including dietary and lifestyle habits that are associated with a cardio-metabolic profile worsening. The presented model allows the study of the processes that leads to acute cardiomyopathy. The mice age used is an important characteristic to be carefully studied, and in our study young animals were used as the metabolic alterations are more easily observed in these animals, even without significant alterations of body weight [36]. Other approaches aimed to study the cardiomyopathy chronic state should be performed to verify more pronounced effects not observed in our study. A potential limitation of our study is the absence of a mechanistic investigation of the diets effects on cardiovascular dysfunction, thus requiring further investigations to clarify the potential mechanisms involved.

## 5. Conclusions

Our results show that high-fat diets and diets rich in salt are able to develop injuries to the cardiovascular system. As an innovation, the present study shows the association of high fat and salt accelerates cardiac and vascular damage in mice. Several references show that special diets, such as high fat, produce the first signs of cardiomyopathy after 20 weeks. After 14 weeks the HFHS diet induces glucose tolerance and insulin sensitivity impairment; hypertension; diastolic dysfunction; an increment in cardiomyocyte size and impaired vascular reactivity. This model helps to characterize the issue by adding the main features of metabolic syndrome, being useful for further studies of cardiometabolic diseases.

## Authors' contribution

Conception and design: LM, VL, MF, VB. Acquisition, analysis and interpretation of data: Mendes-Junior; Freitas-Lima; Lima; Braga; Oliveira; J.R; Santos S. Analysis of data: Mendes-Junior; Freitas-Lima; Lima; Melo; Braga; Campagnole-Santos; Santos S. Materials and reagents: Guimarães; De Paula; Melo; Campagnole-Santos; Santos R; Santos S. Review and approval: Mendes-Junior; Freitas-Lima; Lima; Oliveira; J.R; Guimarães; De Paula; Melo; Campagnole-Santos; Santos R; Braga; Santos S.

## Conflict of interest

The authors declare that this research was conducted in the absence of any commercial or financial relationships that could be considered as a potential conflict of interest.

## Acknowledgements

The authors thank Webster Glayser Pimenta dos Reis for his technical assistance in experimental procedures. Histological procedures were performed at the Multiuser Laboratory of Molecular Histology and Immunohistochemistry facilities of the Health Sciences Center of the Federal University of Espirito Santo.

## Funding

This work was partially supported by the following institutions: Coordenadoria de Aperfeiçoamento do Pessoal de Nível Superior (CAPES), Conselho Nacional de Desenvolvimento Científico e Tecnológico (CNPq) and Fundação de Amparo à Pesquisa de Minas

Gerais (FAPEMIG).

## References

- [1] J.E. Kanter, K.E. Bornfeldt, Impact of diabetes mellitus, *Arterioscler. Thromb. Vasc. Biol.* 36 (6) (2016 Jun) 1049–1053 (PubMed PMID: 27225786. PubMed Central PMCID: Pmc4972454. Epub 2016/05/27. eng).
- [2] D. Dallmeier, M.G. Larson, R.S. Vasan, J.F. Keaney Jr., J.D. Fontes, J.B. Meigs, et al., Metabolic syndrome and inflammatory biomarkers: a community-based cross-sectional study at the Framingham Heart Study, *Diabetol. Metab. Syndr.* 4 (1) (2012 Jun 20) 28 (PubMed PMID: 22716219. PubMed Central PMCID: Pmc3547735. Epub 2012/06/22. eng).
- [3] L.C. Freitas Lima, V.A. Braga, M. do Socorro de Franca Silva, J.C. Cruz, S.H.S. Sousa Santos, M.M. de Oliveira Monteiro, et al., Adipokines, diabetes and atherosclerosis: an inflammatory association, *Front. Physiol.* 6 (2015) 304 (PubMed PMID: 26578976. PubMed Central PMCID: Pmc4630286. Epub 2015/11/19. eng).
- [4] M.T. Waddingham, A.J. Edgley, H. Tsuchimochi, D.J. Kelly, M. Shirai, J.T. Pearson, Contractile apparatus dysfunction early in the pathophysiology of diabetic cardiomyopathy, *World J. Diabetes* 6 (7) (2015 Jul 10) 943–960 (PubMed PMID: 26185602. PubMed Central PMCID: Pmc4499528. Epub 2015/07/18. eng).
- [5] J.K. Kim, H.J. Kim, S.Y. Park, A. Cederberg, R. Westergren, D. Nilsson, et al., Adipocyte-specific overexpression of FOXC2 prevents diet-induced increases in intramuscular fatty acyl CoA and insulin resistance, *Diabetes* 54 (6) (2005 Jun) 1657–1663 (PubMed PMID: 15919786. Epub 2005/05/28. eng).
- [6] R.E. Brainard, L.J. Watson, A.M. Demartino, K.R. Brittan, R.D. Readnow, A.A. Boakye, et al., High fat feeding in mice is insufficient to induce cardiac dysfunction and does not exacerbate heart failure, *PLoS One* 8 (12) (2013) e83174 (PubMed PMID: 24367585. PubMed Central PMCID: Pmc3867436. Epub 2013/12/25. eng).
- [7] Q. Yu, D.F. Larson, D. Slayback, T.F. Lundeen, J.H. Baxter, R.R. Watson, Characterization of high-salt and high-fat diets on cardiac and vascular function in mice, *Cardiovasc. Toxicol.* 4 (1) (2004) 37–46 (PubMed PMID: 15034204. Epub 2004/03/23. eng).
- [8] M.V. Costa, C. Fernandes-Santos, S. Faria Tda, M.B. Aguilu, C.A. Mandarim-de-Lacerda, Diets rich in saturated fat and/or salt differentially modulate atrial natriuretic peptide and renin expression in C57BL/6 mice, *Eur. J. Nutr.* 51 (1) (2012 Feb) 89–96 (PubMed PMID: 21499941. Epub 2011/04/19. eng).
- [9] G. Boden, P. She, M. Mozzoli, P. Cheung, K. Gumireddy, P. Reddy, et al., Free fatty acids produce insulin resistance and activate the proinflammatory nuclear factor-kappaB pathway in rat liver, *Diabetes* 54 (12) (2005 Dec) 3458–3465 (PubMed PMID: 16306362. Epub 2005/11/25. eng).
- [10] R. Buettner, J. Scholmerich, L.C. Bollheimer, High-fat diets: modeling the metabolic disorders of human obesity in rodents, *Obesity (Silver Spring, Md)* 15 (4) (2007 Apr) 798–808 (PubMed PMID: 17426312. Epub 2007/04/12. eng).
- [11] T.A. Lutz, S.C. Woods, Overview of animal models of obesity, *Curr. Protoc. Pharmacol.* (2012 Sep), <https://doi.org/10.1002/0471141755.ph0561s58> (Chapter 5:Unit5.61. PubMed PMID: 22948848. PubMed Central PMCID: Pmc3482633. Epub 2012/09/06. eng).
- [12] M. Wang, E.G. Lakatta, The salted artery and angiotensin II signaling: a deadly duo in arterial disease, *J. Hypertens.* 27 (1) (2009 Jan) 19–21 (PubMed PMID: 19050444. PubMed Central PMCID: Pmc3091136. Epub 2008/12/04. eng).
- [13] M. Osterholt, T.D. Nguyen, M. Schwarzer, T. Doentz, Alterations in mitochondrial function in cardiac hypertrophy and heart failure, *Heart Fail. Rev.* 18 (5) (2013 Sep) 645–656 (PubMed PMID: 22968404. Epub 2012/09/13. eng).
- [14] E. Ferrannini, G. Buzzigoli, R. Bonadonna, M.A. Giorico, M. Oleggini, L. Graziadei, et al., Insulin resistance in essential hypertension, *N. Engl. J. Med.* 317 (6) (1987 Aug 6) 350–357 (PubMed PMID: 3299096. Epub 1987/08/06. eng).
- [15] E.J. Gallagher, D. Leroith, E. Karnieli, Insulin resistance in obesity as the underlying cause for the metabolic syndrome, *Mt. Sinai J. Med. N. Y.* 77 (5) (2010 Sep–Oct) 511–523 (PubMed PMID: 20960553. Epub 2010/10/21. eng).
- [16] K. Rahmouni, D.A. Morgan, G.M. Morgan, X. Liu, C.D. Sigmund, A.L. Mark, et al., Hypothalamic PI3K and MAPK differentially mediate regional sympathetic activation to insulin, *J. Clin. Invest.* 114 (5) (2004 Sep) 652–658 (PubMed PMID: 15343383. PubMed Central PMCID: Pmc514588. Epub 2004/09/03. eng).
- [17] D. Tripathy, P. Mohanty, S. Dhindsa, T. Syed, H. Ghanim, A. Aljada, et al., Elevation of free fatty acids induces inflammation and impairs vascular reactivity in healthy subjects, *Diabetes* 52 (12) (2003 Dec) 2882–2887 (PubMed PMID: 14633847. Epub 2003/11/25. eng).
- [18] A.J. Kennedy, K.L. Ellacott, V.L. King, A.H. Hasty, Mouse models of the metabolic syndrome, *Dis. Model. Mech.* 3 (3–4) (2010 Mar–Apr) 156–166 (PubMed PMID: 20212084. PubMed Central PMCID: Pmc2869491. Epub 2010/03/10. eng).
- [19] S. Boudina, E.D. Abel, Diabetic cardiomyopathy, causes and effects, *Rev. Endocr. Metab. Disord.* 11 (1) (2010 Mar) 31–39 (PubMed PMID: 20180026. PubMed Central PMCID: Pmc2914514. Epub 2010/02/25. eng).
- [20] R.B. Devereux, M.J. Roman, M. Paranicas, M.J. O'Grady, E.T. Lee, T.K. Welty, et al., Impact of diabetes on cardiac structure and function: the strong heart study, *Circulation* 101 (19) (2000 May 16) 2271–2276 (PubMed PMID: 10811594. Epub 2000/05/16. eng).
- [21] E. Dirckx, R.W. Schwenk, J.F. Glatz, J.J. Luiken, G.J. van Eys, High fat diet induced diabetic cardiomyopathy, *Prostaglandins Leukot. Essent. Fat. Acids* 85 (5) (2011 Nov) 219–225 (PubMed PMID: 21571515. Epub 2011/05/17. eng).
- [22] T. Saritas, E. Tascilar, A. Abaci, Y. Yozgat, M. Dogan, R. Dundaroz, et al., Importance of plasma N-terminal pro B-type natriuretic peptide, epicardial adipose tissue, and carotid intima-media thicknesses in asymptomatic obese children, *Pediatr. Cardiol.* 31 (6) (2010 Aug) 792–799 (PubMed PMID: 20419296).

- [23] M. Boyraz, O. Pirgon, B. Akyol, B. Dundar, F. Cekmez, N. Eren, Importance of epicardial adipose tissue thickness measurement in obese adolescents, its relationship with carotid intima-media thickness, and echocardiographic findings, *Eur. Rev. Med. Pharmacol. Sci.* 17 (24) (2013 Dec) 3309–3317 (PubMed PMID: 24379061).
- [24] D.N. Ferreira, I.A. Katayama, I.B. Oliveira, K.T. Rosa, L.N. Furukawa, M.S. Coelho, et al., Salt-induced cardiac hypertrophy and interstitial fibrosis are due to a blood pressure-independent mechanism in Wistar rats, *J. Nutr.* 140 (10) (2010 Oct) 1742–1751 (PubMed PMID: 20724490). Epub 2010/08/21. eng).
- [25] S. Cosson, J.P. Kevorkian, Left ventricular diastolic dysfunction: an early sign of diabetic cardiomyopathy? *Diabete Metab.* 29 (5) (2003 Nov) 455–466 (PubMed PMID: 14631322). Epub 2003/11/25. eng).
- [26] B. Pirat, W.A. Zoghbi, Echocardiographic assessment of left ventricular diastolic function, *Anadolu kardioloji dergisi: AKD = Anatol. J. Cardiol.* 7 (3) (2007 Sep) 310–315 (PubMed PMID: 17785223). Epub 2007/09/06. eng).
- [27] L. Maya, F.J. Villarreal, Diagnostic approaches for diabetic cardiomyopathy and myocardial fibrosis, *J. Mol. Cell. Cardiol.* 48 (3) (2010 Mar) 524–529 (PubMed PMID: 19595694). Pubmed Central PMCID: Pmc2824060. Epub 2009/07/15. eng).
- [28] K.C. Chang, C.D. Tseng, T.F. Chou, Y.L. Cho, T.C. Chi, M.J. Su, et al., Arterial stiffening and cardiac hypertrophy in a new rat model of type 2 diabetes, *Eur. J. Clin. Investig.* 36 (1) (2006 Jan) 1–7 (PubMed PMID: 16403003). Epub 2006/01/13. eng).
- [29] R.H. Ritchie, J.E. Love, K. Huynh, B.C. Bernardo, D.C. Henstridge, H. Kiriazis, et al., Enhanced phosphoinositide 3-kinase(p110alpha) activity prevents diabetes-induced cardiomyopathy and superoxide generation in a mouse model of diabetes, *Diabetologia* 55 (12) (2012 Dec) 3369–3381 (PubMed PMID: 23001375). Epub 2012/09/25. eng).
- [30] M.A. Delbin, A.J. Trask, The diabetic vasculature: physiological mechanisms of dysfunction and influence of aerobic exercise training in animal models, *Life Sci.* 102 (1) (2014 Apr 25) 1–9 (PubMed PMID: 24583313). Epub 2014/03/04. eng).
- [31] B. Candemir, F.S. Ertas, C. Ozdol, C.T. Kaya, M. Kilickap, O. Akyurek, et al., Effect of hypertension on coronary remodeling patterns in angiographically normal or minimally atherosclerotic coronary arteries: an intravascular ultrasound study, *Clin. Exp. Hypertens.* (New York, NY: 1993) 34 (6) (2012) 432–438 (PubMed PMID: 22502594). Epub 2012/04/17. eng).
- [32] T.D. Reil, R.J. Barnard, V.S. Kashyap, C.K. Roberts, H.A. Gelabert, Diet-induced changes in endothelial-dependent relaxation of the rat aorta, *J. Surg. Res.* 85 (1) (1999 Jul) 96–100 (PubMed PMID: 10383844). Epub 1999/06/29. eng).
- [33] M.A. Boegehold, The effect of high salt intake on endothelial function: reduced vascular nitric oxide in the absence of hypertension, *J. Vasc. Res.* 50 (6) (2013) 458–467 (PubMed PMID: 24192502). Epub 2013/11/07. eng).
- [34] H.D. Intengan, E.L. Schiffrin, Vascular remodeling in hypertension: roles of apoptosis, inflammation, and fibrosis, *Hypertension* (Dallas, Tex: 1979) 38 (3 Pt 2) (2001 Sep) 581–587 (PubMed PMID: 11566935). Epub 2001/09/22. eng).
- [35] M.J. Mulvany, Small artery remodelling in hypertension: causes, consequences and therapeutic implications, *Med. Biol. Eng. Comput.* 46 (5) (2008 May) 461–467 (PubMed PMID: 18228071). Epub 2008/01/30. eng).
- [36] M. Tschop, M.L. Heiman, Rodent obesity models: an overview, *Exp. Clin. Endocrinol. Diabetes Off. J. Ger. Soc. Endocrinol. Ger. Diabetes Assoc.* 109 (6) (2001) 307–319 (PubMed PMID: 11571668). Epub 2001/09/26. eng).
- [37] T.A. Pinheiro, A.S. Barcala-Jorge, et al., Obesity and malnutrition similarly alter the renin-angiotensin system and inflammation in mice and human adipose, *J. Nutr. Biochem.* 48 (2017) 74–82, <https://doi.org/10.1016/j.jnutbio.2017.06.008> (PMID: 28779634).
- [38] A. Daugherty, D. Rateri, L. Hong, A. Balakrishnan, Measuring blood pressure in mice using volume pressure recording, a tail-cuff method, *J. Vis. Exp.* 15 (27) (2009), <https://doi.org/10.3791/1291> (pii: 1291. PMID: 19488026).